

Mass wasting on the submarine Lomonosov Ridge, central Arctic Ocean

Yngve Kristoffersen^{a,*}, Bernard J. Coakley^b, John K. Hall^c, Margo Edwards^d

^a Department of Earth Science, University of Bergen, N-5007 Bergen, Norway

^b Department of Geology and Geophysics, University of Alaska, Fairbanks, AK 99775-5780, USA

^c Geological Survey of Israel, Jerusalem 95501, Israel

^d Hawaii Mapping Research Group, Hawaii Institute of Geophysics and Planetology, University of Hawaii, Honolulu, Hawaii, USA

Received 28 October 2006; received in revised form 4 April 2007; accepted 13 April 2007

Abstract

A total of seven arcuate transverse troughs 5–6 km wide, 7–9 km long and 150–200 m deep are present on both sides of the crest of the central part of Lomonosov Ridge, Arctic Ocean. The troughs occur within a restricted ridge length of ca. 65 km. Trough morphology and disrupted, piecewise continuous sub-bottom reflections down to a common stratigraphic horizon below the troughs indicate lateral spread of progressively disintegrating sediment blocks above a glide plane. Lomonosov Ridge is aseismic, but the spatially restricted mass waste occurrences suggest sediment instability induced by earthquake loading. Another possibility is a pressure wave from a possible impact of an extraterrestrial object on Alpha Ridge about 500 km away. The slide event(s) is likely to be pre-late Pleistocene as sediment deposition within one of the slide scars appears continuous over the last c. 600 ka. © 2007 Elsevier B.V. All rights reserved.

Keywords: Arctic Ocean; Lomonosov Ridge; seismic reflection; slide scars; mass wasting

1. Introduction

Hemipelagic clays and biogenic particulate matter in the water column accumulate as a uniform drape on submarine plateaus and ridges in the abyssal realm (Figs. 1 and 2). Bottom currents may shape, attenuate or partly remove sediment accumulations. However, local disruption of stratal continuity and absence of the upper parts of a 450 m thick hemi-pelagic section in an aseismic and low energy bottom current environment on the crest of Lomonosov Ridge, central Arctic Ocean between

86°–87° N latitude, is intriguing. We use swath bathymetry and seismic reflection data to outline the aerial extent and identify the nature of these bed form truncations in order to investigate the underlying geological processes.

2. Geological and oceanographic setting

Lomonosov Ridge is a submarine feature of alpine proportions which rises 3 km above the adjacent abyssal plains (Jakobsson et al., 2000). The 50–100 km wide and more than 1500 km long structure comprises an en-echelon series of fault blocks on the Siberian end and more parallel tectonic structures on the Greenland end of the ridge (Cochran et al., 2006). Seismic reflection data across the flat-topped central part of the ridge (Fig. 2) show an upper unit ca. 420 m thick, of hemipelagic

* Corresponding author. Tel.: +47 55583407; fax: +47 55583660.

E-mail address: yngve.kristoffersen@geo.uib.no
(Y. Kristoffersen).

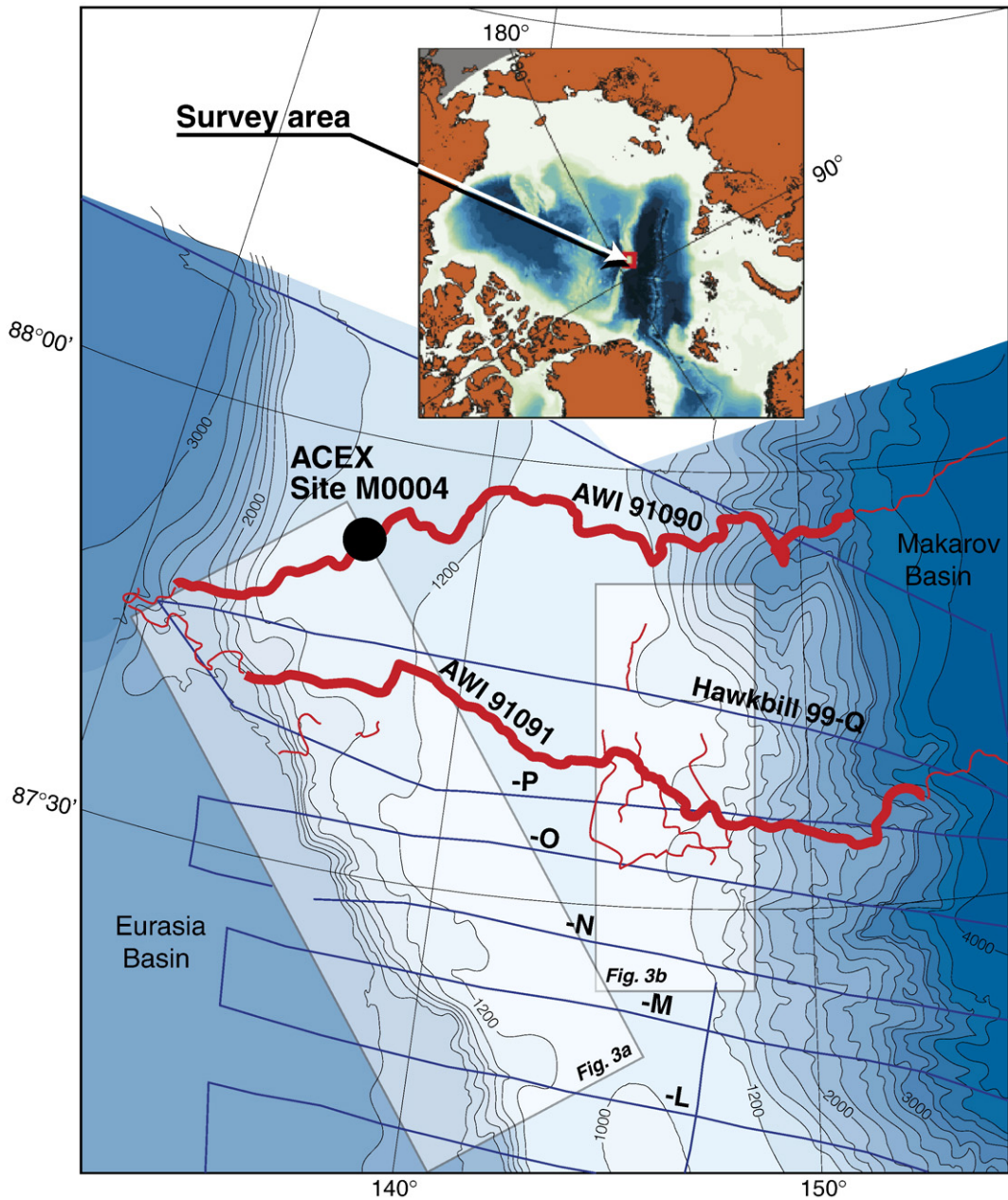


Fig. 1. Site survey area on the central part of Lomonosov Ridge, Arctic Ocean (red square in insert map) with location of multi-channel seismic lines acquired from icebreakers in 1991 and 2001 (red lines) as well as chirp sonar measurements (blue lines) made from nuclear submarine *Hawkbill* (SCICEX). Bathymetry is derived from multi-beam measurements made by *Hawkbill* (blue tracks) and compiled from charts available at http://www.soest.hawaii.edu/HMRG/Aagruuk/SCICEX/Surveys1999/Lomonosov99_Bathymetry_16_27.htm. Contour interval 200 m. Heavy red lines show the portions of the seismic lines AWI 91090 and -91091 where the acoustic stratigraphy across Lomonosov Ridge is shown as line drawings in Fig. 2. Arctic Coring Expedition drill site M0004 marked by large black dot. (For interpretation of the references to colour in this figure legend, the reader is referred to the web version of this article.)

draped above a peneplaned surface that represents an unconformity (Kiselev, 1970; Jokat et al., 1992). The peneplain indicates that the ridge crest had been at or above sea level and subsequently subsided to receive the

hemipelagic drape. Plate tectonic arguments and geophysical data strongly suggest the ridge represents a sliver of the Barents/Kara Sea continental shelf that was rifted off during the late Paleocene (Wilson, 1963; Jokat

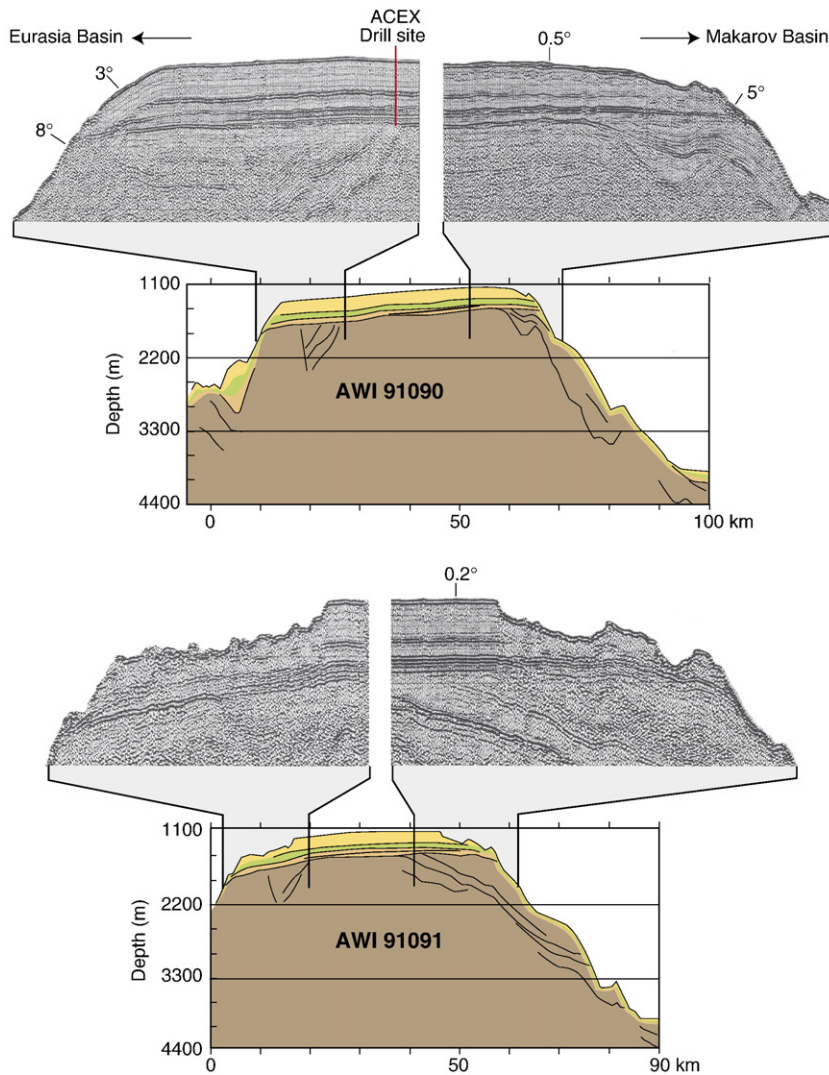


Fig. 2. Line drawing of two seismic transects (line AWI 91090 and -91091 in Fig. 1) across Lomonosov Ridge with details of the acoustic stratigraphy in the vicinity of the ridge perimeter. The positions of transects are marked by heavy red lines in Fig. 1. Slope angles along Line AWI 91090 are indicated in the upper panel. (For interpretation of the references to colour in this figure legend, the reader is referred to the web version of this article.)

et al., 1992; Brozena et al., 2003). The underlying rocks are prograded towards the Makarov Basin on the south side of the ridge while the Eurasia Basin side is characterized by truncated infill in half-grabens (Jokat et al., 1992). Scientific drilling by the Arctic Coring Expedition on the crest of the ridge near 88° N (Fig. 1) encountered late Paleocene/Early Eocene hard silty clay/mudstone unconformably overlying Campanian shallow marine sand, sandstone and mudstone (Shipboard Scientific Party, 2005; Moran et al., 2006).

Hemipelagic deposition will be influenced by the bottom current regime. The intermediate water of the Arctic Ocean extends from ca. 200 m down to

1500–1700 m below sea level which brackets the crest of Lomonosov Ridge (Rudels et al., 1994). The intermediate water consists primarily of inflow from the Atlantic via the Fram Strait and the Barents Sea. The thermo-haline driven circulation forms a boundary current which follows the circum-polar continental margin and also includes separate gyres in the Eurasia, Makarov and Canada basins (Rudels et al., 1994). Water flows east along the north side of Lomonosov Ridge at velocities of < 5 cm/s (Rudels et al., 1994; Woodgate et al., 2001) and pulses across the ridge at velocities that exceed 10 cm/s (Aagard, 1981). Flow is towards the west on the Makarov Basin side of Lomonosov Ridge. The relatively sluggish

bottom current regime does not appear to have facilitated significant sediment redistribution or preferential deposition within the time span less than a few million years captured by the available piston cores or high resolution seismic data (Blasco et al., 1979; Jakobsson, 1999; Kristoffersen et al., 2004).

3. Data

Multi-channel seismic reflection data collected by research icebreaker *Polarstern* in 1991 initially defined the acoustic stratigraphy of Lomonosov Ridge (Jokat et al., 1992). Additional reflection data was acquired by icebreaker *Oden* in an attempted site survey grid in 2001 (Kristoffersen, 2001). Swath bathymetry and high resolution seismic (chirp sonar) data have also been collected over the Lomonosov Ridge by site surveys in preparation for scientific drilling using transducers mounted on the hull of U.S. nuclear submarine *Hawkbill* in 1999 (Edwards and Coakley, 2003). The contrasting regularity between track lines of the submarine and ice-breaking surface vessels illustrates the extreme difficulty of completing a site survey grid in a 8–9/10 cover of 2–3 m thick sea ice (Fig. 1). Diesel driven icebreakers have to follow patchy leads of opportunity and any regularity of the grid is a result of fortunate weather conditions. The seismic data were acquired with two 3 l Bolt guns (*Polarstern*) and two 4 l G-guns (*Oden*) as seismic sources and recorded with a 12 channel, 300 m long (*Polarstern*) and an 8 channel, 200 m long hydrophone cable towed 100 m behind the vessel (*Oden*). Source depth varied from 8 m below the sea surface to shooting in the air, and streamer depth ranged from 0–100 m, but usually 5–10 m, depending of ship's speed. In heavy sea ice, the average survey speed was about 2 knots because the vessel lost momentum about every 200 m (*Oden*) on average. The shot files were edited for particularly noisy traces and band pass filtered. The data was binned and stacked using velocities derived from sonobuoy measurements (Jokat et al., 1995a) and a band pass filter applied before display. Optimum stacking velocities can not be obtained from multi-channel data from this region, because the need for frequent and rapid recovery renders hydrophone cables longer than 300 m impractical unless ice conditions are exceptionally light. The quality of the processed data is relatively good (Fig. 2) in spite of considerable disadvantages such as ambient noise levels 3–5 times higher than the open ocean environment (Jokat et al., 1995b), low data fold as well as inadequate depth control of source and receiver. The nuclear submarine *Hawkbill* collected swath bathymetry and chirp sonar data at 16 knots. Cross-

correlation of the 50 ms long and 2.7–6.7 kHz sweep achieved a resolution of 0.3 m and an image of the acoustic layering of the upper 50 m of soft sediments.

4. Results

The morphology of Lomonosov Ridge at 86°–87° N is characterized by a 25–40 km wide level crest bounded towards the Eurasia Basin by a steep slope (up to 16°) containing few indentations. In contrast the more gentle sloping (<8°) Makarov Basin side of the ridge has many incisions (Figs. 1–3). Tributaries on the upper slope of the Makarov Basin side of the ridge feed into broader, more than 300 m deep valleys on the lower slope. Three transverse crescent-shaped troughs on the ridge crest, each 7–9 km long and 5–6 km wide, face the Makarov Basin and four similar troughs face the Eurasia Basin along the perimeter of the crestal region of Lomonosov Ridge. The troughs are 150–200 m deep and project down into some of the numerous incisions on the Makarov Basin side of the ridge while the upper slope is relatively smooth on the Eurasia Basin side (Figs. 1 and 3). High resolution chirp- and multi-channel seismic reflection profiles crossing into the troughs demonstrate local truncations of the uppermost part of the acoustically well stratified 450 m thick hemipelagic drape. The head of the troughs form 50–100 m high scarps with declivities of as much as 25° (Fig. 3). Sediments within the troughs seaward of the scarps are disturbed with few patches of continuous acoustic reflections above a common stratigraphic level corresponding to the top of a band of high amplitude reflections (Fig. 4). A hummocky seafloor within the troughs is resolved in the chirp sonar data (Fig. 3). In contrast, the stratigraphy of the flanks of Lomonosov Ridge outside the troughs appears complete and undisturbed (Fig. 2, line AWI 91090 and Fig. 3B, line *Hawkbill* 99-N).

5. Interpretation

A consistent and characteristic morphology for the troughs constrains possible mechanisms for their origin. The disrupted and missing stratigraphic section within the troughs clearly demonstrates local sediment removal (Figs. 2, 3 and 4). Possible agents capable of removing large volumes of sediments are bottom currents, grounded deep draft ice or gravitational mass wasting events. Sediment instability may be generated by bottom currents undercutting the upper slope, the presence of gas/gas hydrates, or different types of loading events such as tides, sea level changes, icebergs and earthquakes.

Sediment redistribution by bottom currents may contribute to slope instability (Kayen et al., 1989). Contour currents along the flanks of Lomonosov Ridge are slow (<5 cm/s) and west-flowing intermediate water crosses the ridge crest from the Eurasia Basin with velocities up to 12 cm/s (Aagard, 1981). These velocities are clearly not capable of redistributing sediments. Eddies with diameter 10–20 km and tangential speeds

>30 cm/s are relatively frequent within the intermediate water, but their vertical extent is limited to less than 500 m (Manley and Hunkins, 1985; Aagard and Carmack, 1994). Also, a cluster of morphologically similar troughs in a restricted area on the ridge is difficult to reconcile with current erosion.

Another possibility is seabed erosion by deep draft ice bergs as observed on Lomonosov Ridge down to a

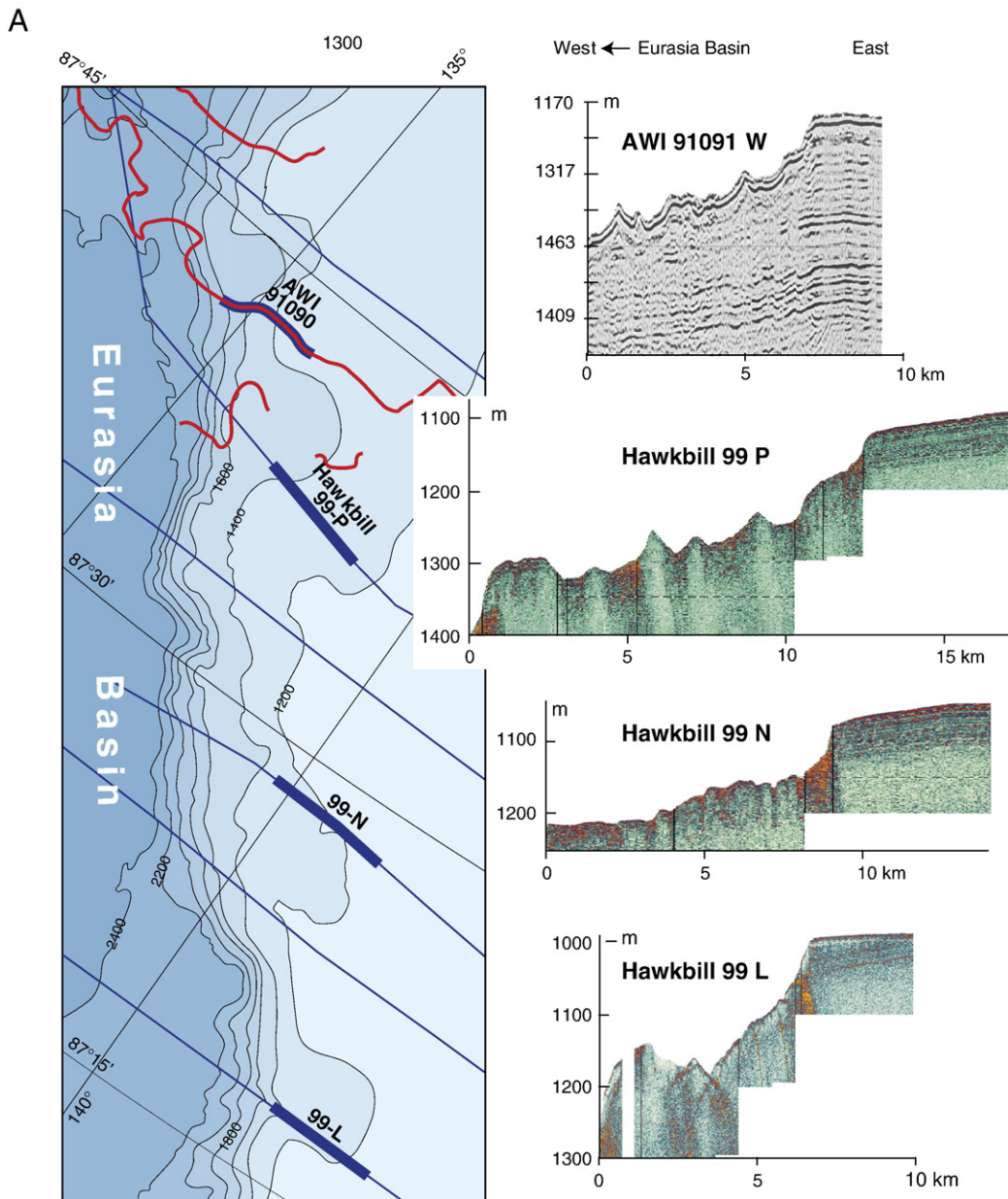


Fig. 3. Acoustic sections and profile locations from the perimeter of Lomonosov Ridge across the main scarps separating undisturbed and disrupted stratigraphy. Areas of the detailed maps are marked by frames in Fig. 1. A) Acoustic sections across the Eurasia Basin side of Lomonosov Ridge. B) Acoustic sections across the Makarov Basin side of Lomonosov Ridge.

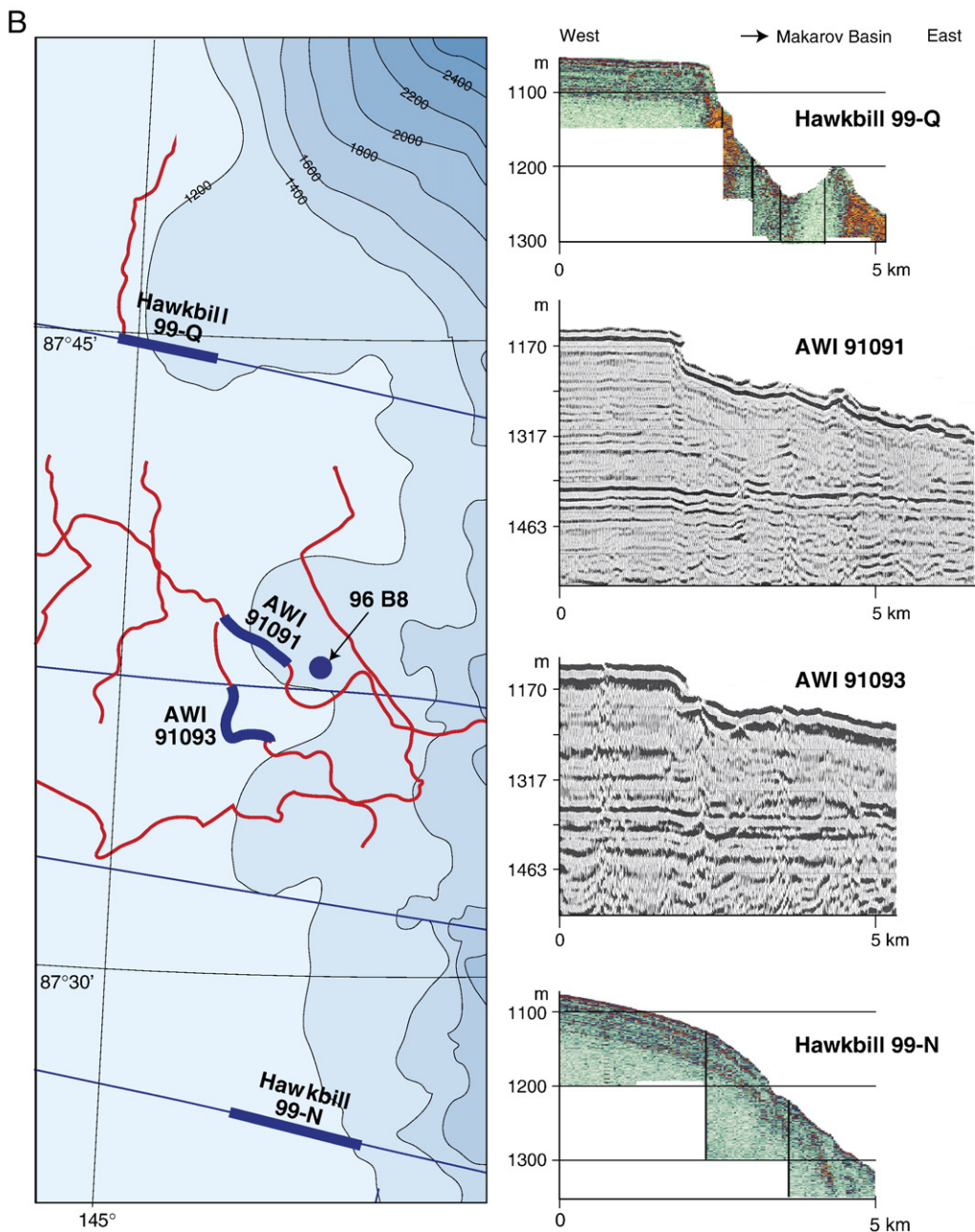


Fig. 3 (continued).

maximum water depth of 970 m (Jakobsson et al., 2001; Polyak et al., 2001; Kristoffersen et al., 2004; Jokat, 2005). All available seismic data from the Lomonosov Ridge show an undisturbed hemi-pelagic drape below 970 m depth including the ridge crest in the area of the troughs (>1060 m depth). Hence, erosion by bottom currents or iceberg keels is not likely to have caused direct excavation of the troughs. More significant are

the morphological characteristics of the troughs; arc-shaped main scarps enclosing hummocky sea bed and disrupted sub-bottom stratigraphy (Fig. 3). Bathymetric profiles that are parallel to the axes of the troughs and perpendicular to the ridge show a tendency toward angular, rather than rounded micro-morphology (Figs. 3 and 4). We interpret this to indicate that the troughs are underlain by rotated blocks of sub-bottom sediments

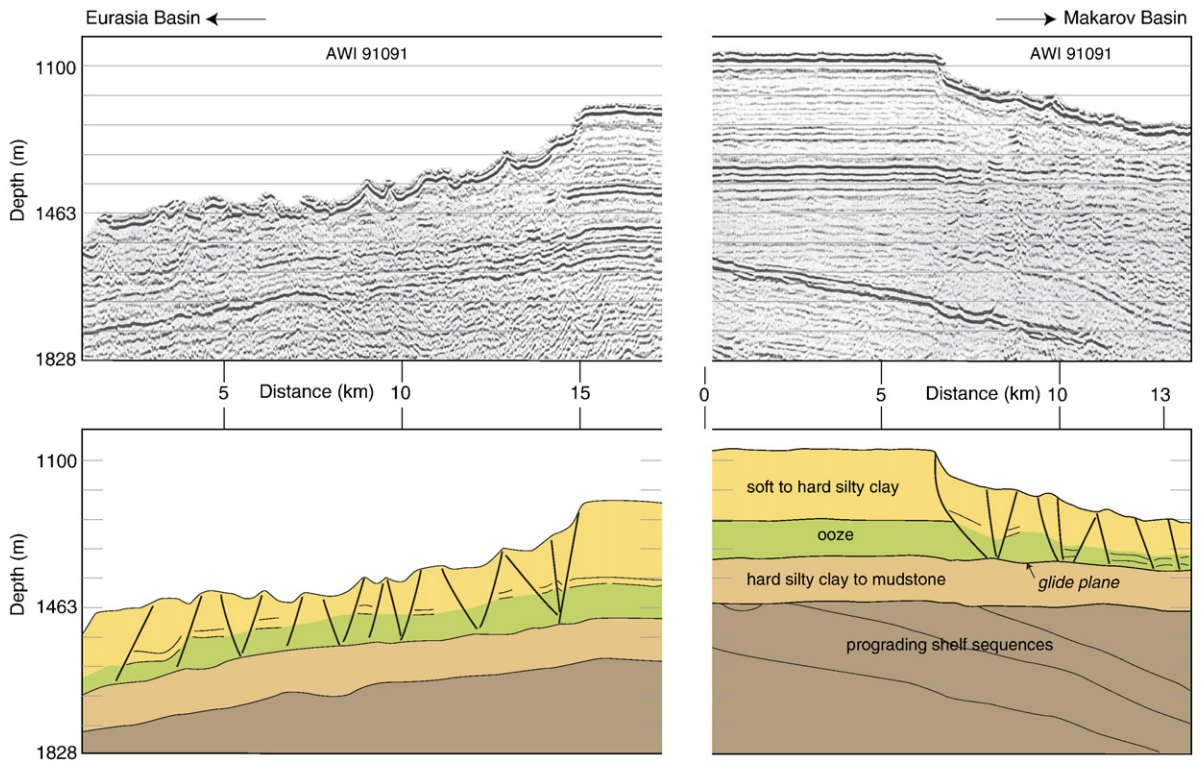


Fig. 4. Detail of the acoustic stratigraphy (line AWI 91091) across the disrupted area (upper panels) and interpreted line drawing (lower panels) including lithostratigraphic information from the ACEX results (Shipboard Scientific Party, 2005). Profile locations shown in Fig. 2 (lower panel) and Fig. 1. The depth-section assumes a velocity of 1463 m/s in the water column and 1800 m/s in the sediments above the unconformity.

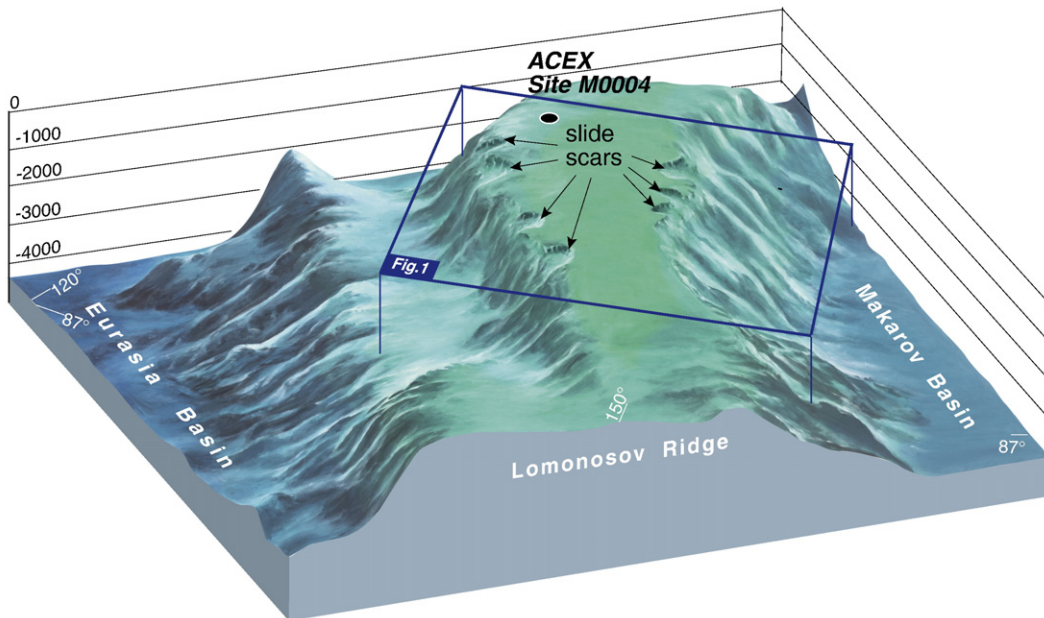


Fig. 5. Perspective model of Lomonosov Ridge topography showing the setting of the slide scars and ACEX drill site M0004. The basic model was generated in GMT (Wessel and Smith, 1991) using the IBCAO data base (Jakobsson et al., 2000) modified by the SCICEX results within the survey area. Shading has been manually enhanced. The site survey area shown in Fig. 1 is framed.

within a sediment rubble field (Fig. 4). Also, the presence of flat reflection segments at depth is likely to reflect slide blocks with partially intact stratigraphy within the slide mass (Fig. 4). The disturbed acoustic stratigraphy in all seismic reflection profiles occurs only above a band of high amplitude reflections about 120 m above the regional unconformity (Fig. 4). This stratigraphic level appears to represent a glide plane (Fig. 4) and corresponds to the transition from pelagic ooze to the underlying more competent hard silty clay to mudstone (Shipboard Scientific Party, 2005). Material within the slide scars appears to have moved by sliding of progressively disintegrating sediment blocks above a basin-dipping glide plane at the base of the ooze and the top of the hard silty clay (Fig. 4). Sliding at each of the present slide scars most likely nucleated on a steep incline on the slope below the mouth of the scar. Local instability may have been created by unloading of the footwall pressure. Once initiated, this process propagated upslope and eventually created a large retrogressive slide. At the mouths of the slide scars, the slide mass accelerated on the increasingly steeper slopes beneath the foot of the troughs and down the upper flanks of Lomonosov Ridge. The lack of down-slope incisions on the sediment starved Eurasia Basin side suggest that the mass wasting event(s) was not associated with significant down-slope erosion (Fig. 3A). However, on the Makarov Basin side, slope valleys form sediment pathways to the deep basin (Fig. 3B). This difference in slope morphology (Figs. 1, 3 and 5) can be explained by slope maturity as the Makarov Basin margin represented the Mesozoic continental margin of polar Europe before Eurasia Basin opened. The Eurasia Basin side of Lomonosov Ridge is sediment starved and is likely to have a substratum of older, more competent rocks.

6. Discussion

6.1. Slide scar morphology and slide mechanism

The angular crests in sea bed morphology within the slide scars as well as associated patchy sub-bottom acoustic reflection segments indicate presence of partially intact sediment blocks (Figs. 3 and 4). Modelling suggests that the form of material transport in a failed volume of sediments depends critically on the degree of strain softening once failure has occurred (Gauer et al., 2005). In the absence of strain softening, deformation by continuous stretching predominates, whereas strain softening favours displacement of intact blocks of sediment within a slide scar. On the Lomonosov Ridge,

the blocks would progressively disintegrate as the material accelerated down-slope.

6.2. Sediment stability and triggers for failure

Slope angles along the perimeter of the crest of Lomonosov Ridge between 87° 15' N and 88° N range from level seabed on the ridge plateau to 6° in water depths less than 400 m deeper than the crest of the plateau (Fig. 2, upper panel).

Sediment stability is determined by a balance between the slope-parallel component of gravity and the resistive forces from sediment shear strength. The ACEX drilling results show the hemipelagic drape on top of Lomonosov Ridge consists of an upper unit 220 m thick silty clay, and a middle unit ca. 93 m thick of biosiliceous, silty clay to ooze and a lowermost unit of silty clay to mudstone (Shipboard Scientific Party, 2005). Deposition rates in the upper and lower units are in the range of 1–3 cm/ka. At this rate the sediments gain sufficient strength by consolidation to be stable. Preliminary results of measurements of the ratio between shear strength and maximum past stress (consolidation index) show values around 0.1 in the upper 130 m below the sea floor (mbsf) suggesting under-consolidation (Shipboard Scientific Party, 2005). Values are higher (0.1–0.4) in the interval 130–210 mbsf, but drop to lower levels in the underlying biosiliceous ooze. Single observations at 238 mbsf and 255 mbsf suggest a consolidation index of 0.15 (Shipboard Scientific Party, 2005). The density decreases sharply at 220 mbsf from 1.7 g/cm³ in biosiliceous silty clay to 1.3 g/cm³ in the underlying biosiliceous ooze and remains below 1.6 g/cm³ to 340 mbsf. Densities in the basal hard silty clay to mudstone are in the range 1.7–2.1 g/cm³ (Shipboard Scientific Party, 2005). Thus geotechnically, the upper part of the sedimentary section on Lomonosov Ridge consists of an upper under-consolidated silty clay unit that rests on low strength biosiliceous ooze, which in turn overlies higher strength hard silty clay to mudstone.

Reduced sediment stability may most efficiently arise from reduction in effective stress by increasing pore pressure from an external event such as earthquake loading or head wall erosion which lowers the resistive force sufficiently for failure to occur. A local increase in pore pressure may result from lateral flow of pore water confined by low permeability clay-dominated layers, by melting of gas hydrates, or by the reduction in porosity caused by alteration of biogenic opal-A to opal-CT. However, fluids are less likely to be trapped in an environment with slow and uniform hemipelagic deposition such as the crest and slope of Lomonosov Ridge. Also

bottom simulating reflectors (BSR's) associated with presence of methane have not been identified on this part of the ridge (Shipboard Scientific Party, 2005). This is also the case for the diffuse acoustic reflection response often associated with opal-A to -CT transition (Volpi et al., 2003; Davies and Clark, 2006; Moran et al., 2006). Thus, it appears less likely that permanent excessive pore pressures have been generated by the above mentioned internal factors on the crest of Lomonosov Ridge. A stronger candidate for reduction of sediment stability on Lomonosov Ridge may be transient excess pore pressures from strain induced by earthquake loading, and once failure has occurred, by strain softening (Kvalstad et al., 2005). Dynamic loading from an earthquake has the duration of seconds to minutes, while excess pore pressure generation may peak days or even years later depending on the hydraulic conditions in the sediments (Biscontin et al., 2004). Their modelling suggests that although the highest pore pressures occur at the base of a homogenous section, the ratio of pore pressure to initial vertical stress is highest in the upper 20 m of such a section. Shear strains, however are largest in the top 10 m and represents the highest potential for development of the initial shear plane. A large slide may nucleate by local unloading of the footwall pressure on the uppermost slope and the increased instability propagates into a larger sediment volume which then fails and more extensive transport occurs.

The occurrence of seven slide scars within a restricted length of about 65 km along both sides of the crest of Lomonosov Ridge appears locally unique for the more than 1500 km long ridge, and suggests a local trigger mechanism. Monitoring of the seismicity of the Arctic Ocean over the last fifty years has not revealed any epicenters in the area discussed here. The nearest documented earthquakes on Lomonosov Ridge are north of the Canadian Arctic Archipelago, more than 700 km away and are generally of magnitude 3 or less (<http://www.seismo.nrcan.gc.ca>; Fig. 1 in Kristoffersen and Mikkelsen, 2006). Gakkel (1958) on the other hand, reported on an incident that was interpreted as a submarine volcanic eruption on Lomonosov Ridge. At 1215 h on November 24, 1956, the position of the Russian ice station *North Pole 3* was 88.25° N, 65.6° W (water depth 1463 m). The crew suddenly felt a strong shock followed by the smell of hydrogen sulphide, an odour which was detected for several hours. This location overlies the top of Lomonosov Ridge about 300 km from the slide area, and suggests that we can not exclude rare earthquake events on any part of the ridge. Our working hypothesis is that grouping of the slide scars as well as the assumed stability conditions of the sediments suggest

failure could have been triggered by one or more earthquakes.

It is worth noting that a comprehensive analysis of known slides on the North Atlantic margins indicates that the majority of slope failures occur in the depth range 1000–1300 m (Hühnerbach et al., 2004). Internal waves may therefore also play a role in some cases.

A more speculative possibility is related to new evidence of extensive local seabed disturbance, erosion and mass wasting within a 200 km×600 km area on Alpha Ridge, central Arctic Ocean (Hall et al., 2006). These features have been proposed to represent a catastrophic event such as impact of an extra-terrestrial object. Slumps involving Cretaceous material recovered in short (<3.5 m) sediment cores at four different locations within or immediately outside the disturbed area are conjectured to have been generated by the pressure wave from the impact. An impact event on Alpha Ridge, about 500 km distant from the study area, could also have destabilized sediments on Lomonosov Ridge (Fig. 5).

6.3. Timing of mass waste event(s)

All but one of the slide scars in our study area occur at depths where the ridge plateau are below the maximum water depth of iceberg erosion (Fig. 3, profile L). The lack of a resolvable sediment drape over all the main scarps testifies to the youthfulness of the mass wasting event(s). Jakobsson et al. (2001) analyzed a piston core raised from the head of one of the slide scars (Fig. 3B, 96/B8-1pc). A magnetic reversal at 3 m depth correlated with magnetic excursion Biwa II, suggests a deposition rate of ~1 cm/ka over the last 300 ka. As no over-consolidated material is reported from the bottom of the 6.54 m long core, we infer from extrapolation of the sedimentation rate that deposition within the slide scar may have been continuous during the last 600 ka, and post-dates the mass waste event(s). We are not able to discriminate between the possibilities of one or several events.

7. Conclusions

The uniform stratigraphy of the ca. 420 m thick hemipelagic drape which covers the central part of Lomonosov Ridge is locally cut on both sides at the ridge perimeter by 150–200 m deep, 5–6 km wide, and 7–9 km long transverse troughs. Acoustic stratigraphic continuity below the troughs is disrupted only down to a common stratigraphic level below which the bedding appears undisturbed. The troughs are considered to represent slide scars. The lithology and physical properties of the

hemipelagic section has been documented by scientific drilling (*Shipboard Scientific Party, 2005*), and the disrupted beds consist of an upper unit of under-consolidated soft to hard silty clay (0–220 mbsf) overlying a low strength biosiliceous ooze. The intact underlying unit consists of hard silty clay to mudstone. The cluster of slide scars suggests triggering by an external local event, an earthquake or possibly a pressure pulse from impact of an extra-terrestrial object on Alpha Ridge about 500 km away. Local instability was most likely created by unloading of footwall pressure. Once initiated, this process propagated upslope and eventually created large retrogressive slides.

Acknowledgement

The data presented here was part of site surveys crucial to the final documentation for approval of ODP proposal 533 for scientific drilling on the Lomonosov Ridge. R/V *Polarstern* of Alfred Wegener Institute for Marine and Polar Research acquired the first data in 1991. Ship time for a site survey in 2001 from icebreaker *Oden* was funded by the Norwegian Petroleum Directorate, Statoil and USSAC, but would not have materialized without the enthusiasm of the third author and a generous grant from the Margaret Kendrick Blodgett Foundation. The Science Ice Exercise (SCICEX) survey was supported by U.S. Navy and the U.S. National Science Foundation. We thank the captains and the crews of *Polarstern*, *Oden* and the U.S. Navy nuclear submarine *Hawkbill* for their seamanship and support. Stimulating discussions with T. Kvalstad and A. Solheim, Norwegian Geotechnical Institute are much appreciated.

References

- Aagard, K., 1981. On the deep circulation in the Arctic Ocean. *Deep-Sea Res.*, Part A 28, 251–268.
- Aagard, K., Carmack, E.C., 1994. The Arctic Ocean and climate: a perspective. In: Johannessen, O., Muench, R.D., Overland, J. (Eds.), *The Polar Oceans and Their Role in Shaping the Global Environment*. Am. Geophys. Union Geophys. Monograph, vol. 85, pp. 5–20.
- Biscontin, G., Pestana, J.M., Nadim, F., 2004. Seismic triggering of submarine slides in soft cohesive soil deposits. *Mar. Geol.* 203, 341–354.
- Blasco, S.M., Bornhold, B.D., Lewis, C.F.M., 1979. Preliminary results of surficial geology and geomorphology studies of the Lomonosov Ridge, central Arctic Basin. *Geol. Surv. Can. Pap.* 79-1C, 73–83.
- Brozna, J.M., Childers, V., Lawver, L.A., Gahagan, L.M., Forsberg, R., Faleide, J.I., Eldholm, O., 2003. New aerogeophysical study of the Eurasian Basin and Lomonosov Ridge: implications for basin development. *Geology* 31, 825–828.
- Cochran, J.R., Edwards, M.H., Coakley, B.J., 2006. Morphology and structure of the Lomonosov Ridge, Arctic Ocean. *Geochem., Geophys., Geosyst.* 7 (5), Q05019. doi:10.1029/2005GC001114.
- Davies, R.J., Clark, I.R., 2006. Submarine slope failure primed and triggered by silica and its diagenesis. *Basin Res.* 18, 339–350.
- Edwards, M., Coakley, B.J., 2003. SCICEX investigations of the Arctic Ocean System. *Chem. Erde* 63, 281–392.
- Gakkel, Y.Y., 1958. Signs of recent submarine volcanic activity in the Lomonosov range. *Priroda* 4, 97–90 (translated from Russian).
- Gauer, P., Kvalstad, T.J., Forsberg, C.F., Bryn, P., Berg, K., 2005. The last phase of the Storegga Slide: simulation of retrogressive slide dynamics and comparison with slide-scar morphology. *Mar. Pet. Geol.* 22, 171–178.
- Hall, J.K., Kristoffersen, Y., Hunkins, K., Ardai, J., Coakley, B., Hopper, J., the Healy 2005 seismic team, 2006. Evidence for an asteroid impact in the central Arctic Ocean. Poster OS53B-1114, Am. Geophys. Union Fall Meeting, San Francisco, Dec. 11–15.
- Hühnerbach, V., Masson, D.G., partners of the COSTA project, 2004. Landslides in the North Atlantic and its adjacent seas: an analysis of their morphology, setting and behaviour. *Mar. Geol.* 213, 343–362.
- Jakobsson, M., 1999. First high-resolution chirp sonar profiles from the central Arctic Ocean reveal erosion of Lomonosov Ridge sediments. *Mar. Geol.* 158, 111–123.
- Jakobsson, M., Cherkis, N., Woodward, J., Coakley, B., Macnab, R., 2000. A new grid of Arctic bathymetry: A significant resource for scientists and mapmakers. *Eos, Trans. - Am. Geophys. Union* 81 (9), p. 89, 93, 96.
- Jakobsson, M., Løvlie, R., Arnold, E.M., Backman, J., Polyak, L., Knutsen, J.O., Musatov, E., 2001. Pleistocene stratigraphy and paleoenvironmental variation from Lomonosov Ridge sediments, central Arctic Ocean, *Global Planet. Change* 31, 1–22.
- Jokat, W., 2005. The sedimentary structure of Lomonosov Ridge between 88° N and 80° N. *Geophys. J. Int.* 163, 698–726.
- Jokat, W., Uenzelmann-Neben, G., Kristoffersen, Y., Rasmussen, T.M., 1992. Lomonosov Ridge — a double-sided continental margin. *Geology* 20, 887–890.
- Jokat, W., Weigelt, E., Kristoffersen, Y., Rasmussen, T., Schöne, T., 1995a. New insights into the evolution of the Lomonosov Ridge and the Eurasia Basin. *Geophys. J. Int.* 122, 378–392.
- Jokat, W., Buravtsev, V. Yu., Miller, H., 1995b. Marine seismic profiling in ice covered regions. *Polarforschung* 64, 9–17.
- Kayen, R.E., Schwab, W.C., Lee, H.J., Torresan, M.E., Hein, J.R., Quinterno, P.J., Levin, L.A., 1989. Morphology of sea-floor landslides on Horizon Guyot: application of steady-state geotechnical analysis. *Deep-Sea Res.* 36, 1817–1839.
- Kiselev, Y.G., 1970. Some of the features of the present morpho-tectonic structure of Lomonosov Ridge based on seismic data. *Morskaya Geol. i. Geoziz.* 1, 123–128 (translated from Russian).
- Kristoffersen, Y., 2001. An ODP-site survey on Lomonosov Ridge during Arctic Ocean 2001. *Swedish Polar Secretariat Yearbook*, pp. 64–66.
- Kristoffersen, Y., Mikkelsen, N., 2006. On sediment deposition and nature of the plate boundary at the junction between the submarine Lomonosov Ridge, Arctic Ocean and the continental margin of Arctic Canada/North Greenland. *Mar. Geol.* 225, 265–278.
- Kristoffersen, Y., Coakley, B., Jokat, W., Edwards, M., Brekke, H., Gjengedal, J., 2004. Seabed erosion on the Lomonosov Ridge, central Arctic Ocean: a tale of deep draft icebergs in the Eurasia Basin and the influence of Atlantic water inflow on iceberg motion? *Paleoceanography* 19, A3006. doi:10.1029/2003PA000985.
- Kvalstad, T.J., Andresen, L., Forsberg, C.F., Bryn, P., Wangen, M., 2005. The Storegga slide: evaluation of triggering sources and slide mechanisms. *Mar. Pet. Geol.* 22, 245–256.

- Manley, T., Hunkins, K., 1985. Meso-scale eddies of the Arctic Ocean. *J. Geophys. Res.* 90 (C3), 4911–4930.
- Moran, K. and 36 others, 2006. The Cenozoic palaeoenvironment of the Arctic Ocean. *Nature* 441/1 June 2006/ doi:10.1038/nature04800, 601–605.
- Polyak, L., Edwards, M., Coakley, B., Jakobsson, M., 2001. Ice shelves in the Pleistocene Arctic Oceans inferred from glacial deep-sea bed forms. *Nature* 410, 453–457.
- Rudels, B., Jones, E.P., Anderson, L., Kattner, G., 1994. On intermediate depth waters of the Arctic Ocean. In: Johannessen, O., Muench, R., Overland, J. (Eds.), *The Role of the Polar Oceans in Shaping the Global Climate*. Geophysical Monographs, vol. 85. Am. Geophys. Union, Washington, D.C., pp. 33–46.
- Shipboard Scientific Party, 2005. Arctic Coring Expedition (ACEX): Paleooceanographic and tectonic evolution of the central Arctic Ocean. IODP Prelim. Rept., 302. <http://iodp.tamu.edu/publications/PR/302PR/302PR.PDF>.
- Volpi, V., Camerlenghi, A., Hillenbrand, C.D., Rebecco, M., Ivaldi, R., 2003. Effects of biogenic silica on sediment compaction and slope stability on the Pacific margin of the Antarctic Peninsula. *Basin Res.* 15, 339–363.
- Wilson, J.T., 1963. Hypothesis of Earth's behaviour. *Nature* 198, 925–929.
- Woodgate, R.A., Aagard, K., Muench, R.D., Gunn, J., Bjørk, G., Rudels, B., Roach, A.T., Schauer, U., 2001. The Arctic Ocean boundary current along the Eurasian slope and the adjacent Lomonosov Ridge: water mass properties, transports and transformations from moored instruments. *Deep-Sea Res. I* 48, 1757–1792.
- Wessel, P., Smith, W., 1991. Free software helps map and display data. *Eos, Trans. - Am. Geophys. Union* 72 (441), 445–446.